RESEARCH PAPER

Inhibition of high glucose-induced inflammatory response and macrophage infiltration by a novel curcumin derivative prevents renal injury in diabetic rats

Yong Pan[1,2]*, Yi Wang[1]*, Lu Cai[1,2,3], Yuepiao Cai[1], Jie Hu[1], Congcong Yu[1], Jianling Li[1], Zhiguo Feng[1], Shulin Yang[4], Xiaokun Li[1,2] and Guang Liang[1,4]

[1]Bioorganic and Medicinal Chemistry Research Center, School of Pharmaceutical Science, Wenzhou Medical College, Wenzhou, China, [2]Chinese-American Research Institute for Diabetic Complications, Wenzhou Medical College, Zhejiang, China, [3]Department of Pediatrics, University of Louisville, Louisville, Kentucky, USA, and [4]College of Chemistry, Nanjing University of Science and Technology, Nanjing, China

BACKGROUND AND PURPOSE

Inflammation is involved in the development and/or progression of many diseases including diabetic complications. Investigations on novel anti-inflammatory agents may offer new approaches for the prevention of diabetic nephropathy. Our previous bioscreening of synthetic analogues of curcumin revealed C66 as a novel anti-inflammatory compound against LPS challenge in macrophages. In this study, we hypothesized that C66 affects high glucose (HG)-induced inflammation profiles *in vitro* and *in vivo* and then prevents renal injury in diabetic rats via its anti-inflammatory actions.

EXPERIMENTAL APPROACH

Primary peritoneal macrophages (MPM), prepared from C57BL/6 mice, were treated with HG in the presence or absence of C66. Diabetes was induced in Sprague–Dawley rats with streptozotocin, and the effects of C66 (0.2, 1.0 or 5.0 mg·kg^{-1}), administered daily for 6 weeks, on plasma TNF-α levels and expression of inflammatory genes in the kidney were assessed.

KEY RESULTS

Pretreatment of MPMs with C66 reduced HG-stimulated production of TNF-α and NO, inhibited HG-induced IL-1β, TNF-α, IL-6, IL-12, COX-2 and iNOS mRNA transcription, and the activation of JNK/NF-kB signalling. *In vivo*, C66 inhibited the increased plasma TNF-α levels and renal inflammatory gene expression, improved histological abnormalities and fibrosis of diabetic kidney, but did not affect the hyperglycaemia in these diabetic rats.

CONCLUSIONS AND IMPLICATIONS

The anti-inflammatory effects of C66 are mediated by inhibiting HG-induced activation of the JNK/NF-κB pathway, rather than by reducing blood glucose in diabetic rats. This novel compound is a potential anti-inflammatory agent and might be beneficial for the prevention of diabetic nephropathy.

Abbreviations

C66, 2*E*,6*E*)-2,6-bis(2-(trifluoromethyl)benzylidene)cyclohexanone; DN, diabetic nephropathy; FITC, fluorescein isothiocyanate; H&E, haematoxylin and eosin; HG, high glucose; iNOS, inducible NOS; LG, low glucose; MCP-1, monocyte chemotactic protein-1; MPMs, mouse peritoneal macrophage; PAS, periodic acid and Schiff solution; STZ, streptozotocin

Introduction

Inflammation is directly associated with the pathogenesis of many human diseases, including atherosclerosis, pulmonary inflammatory diseases, diabetic complications and cancers (Navarro-Gonzalez and Mora-Fernandez, 2008; Brevetti *et al*., 2010; Kwong *et al*., 2011). Cellular events of inflammatory responses are associated with the activation of the NF-κB (Jeon *et al*., 2010). In addition to LPS, a number of stimuli, including high glucose (HG), have been reported to increase the levels of cellular NF-κB activation, resulting in pro-inflammatory responses and the release of a large amount of inflammatory cytokines (Lee *et al*., 2008; Stan *et al*., 2011), which, within a complex regulatory network, are related to specific immunological processes that promote chronic inflammation and tissue destruction (Lee *et al*., 2008; Navarro-Gonzalez and Mora-Fernandez, 2008; Kopf *et al*., 2010; Kwong *et al*., 2011). Hyperglycaemia induces the *in vivo* inflammatory cascade and therefore plays an important role in the development and progression of diabetic complications (Kaul *et al*., 2010; Kopf *et al*., 2010; Stan *et al*., 2011). Increasingly evidence suggests that inflammatory mechanisms, such as macrophage infiltration and overexpression of proinflammatory cytokines, contribute to the pathogenesis of diabetic nephropathy (Goldberg, 2009; Donath *et al*., 2010; Tang *et al*., 2010; Zong *et al*., 2010). Therefore, investigating anti-inflammatory strategies using anti-inflammatory agents may offer new approaches for treating diabetic nephropathy (DN).

Curcumin (1,7-bis-(4-hydroxy-3-methoxyphenyl)-1,6-heptadiene-3,5-dione) is the main active component of turmeric isolated from the plant *Curcuma longa* L. Curcumin has been extensively demonstrated as a multifunctional molecule with significant regulatory effects on cancer, inflammation and inflammatory related diseases (Morimoto *et al*., 2008; Epstein *et al*., 2010). However, curcumin has one vital drawback, poor bioavailability, which limits its development as a potential therapeutic agent (Garcea *et al*., 2004; Epstein *et al*., 2010). Recent studies showed that the presence of the β-diketone moiety renders it to be rapidly metabolized (Rosemond *et al*., 2004). Designing synthetic structural analogues without the β-diketone moiety is one approach to overcome the poor bioavailability while retaining, or further enhancing, its drug-like effects (Anand *et al*., 2007). In our previous studies, we designed and synthesized of a series of curcumin mono-carbonyl analogues, which exhibited improved pharmacokinetic profiles *in vivo* (Liang *et al*., 2009a). Subsequently, we evaluated more than 100 analogues for their anti-inflammatory properties using LPS-stimulated mouse J774.1A or RAW264.7 macrophages (Liang *et al*., 2008; 2009b; Zhao *et al*., 2010). Amongst these analogues, (2*E*,6*E*)-2,6-bis(2-(trifluoromethyl)benzylidene)cyclohexanone (C66, in

Figure 1) showed a strong inhibitory effect on LPS-induced TNF-α and IL-6 release in mouse macrophages (Liang *et al*., 2009b). In this study, we showed that C66 is able to reduce HG-induce inflammation profiles both *in vitro* and *in vivo*, and then prevent renal injury in experimental diabetic rats via its anti-inflammatory actions.

Methods

Reagents

Glucose, curcumin and mannitol were purchased from Sigma (St. Louis, MO, USA). Compound C66 was synthesized and characterized as described in our previous publication (Liang *et al*., 2009b). Before using it for biological experiments, compound C66 was recrystallized from $CHCl_3$/EtOH, and then HPLC method was used to determine its purity (99.16%). The structures of curcumin and C66 are shown in Figure 1. C66 was dissolved in DMSO for *in vitro* experiments and was dissolved in 1% CMC-Na for *in vivo* experiments. Anti-actin antibody was purchased from Santa Cruz (Santa Cruz, CA, USA); anti-p-IκBα, anti-IKK, anti-p-p65, p-JNK, JNK and anti-CD68 are from Cell Signalling (Danvers, MA, USA).

Animals

Male C57BL/6 mice ($n = 57$) weighing 18–22 g and Sprague–Dawley (SD) rats ($n = 38$) aged 5 weeks were obtained from the Animal Centre of Wenzhou Medical College (Wenzhou, China). Animals were housed at a constant room temperature

curcumin

Delete the β-diketone moiety to obtain the structurally stable mono-carbonyl analogues

C66: (2E,6E)-2,6-bis(2-(trifluoromethyl)benzylidene)cyclohexanone
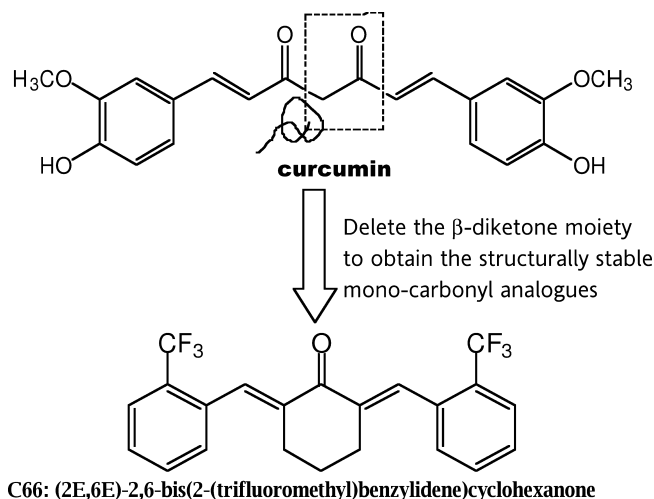
Figure 1

Chemical structures of curcumin and C66.

with a 12:12 h light–dark cycle and fed with a standard rodent diet and water. The animals were acclimatized to the laboratory for at least 3 days before used. All animal care and experimental procedures complied with the 'The Detailed Rules and Regulations of Medical Animal Experiments Administration and Implementation' (Order NO. 1998-55, Ministry of Public Health, China.), and 'Ordinance in Experimental Animal Management' (Order NO. 1998-02, Ministry of Science and Technology, China), and were approved by the Wenzhou Medical College Animal Policy and Welfare Committee (Approval Document NO. 2009/APWC/0031).

Protocols involving the use of animals were approved by the Wenzhou Medical College Animal Policy and Welfare Committee.

Mouse primary peritoneal macrophage (MPM) preparation and culture

C57BL/6 mice were stimulated by an i.p. injection of 6% thioglycollate solution (0.3 g beef extract, 1 g tryptone, 0.5 g NaCl dissolved in 100 mL ddH$_2$O, and filtrated through 0.22 μm filter membrane, 3 mL per mouse) and kept in a pathogen-free condition for 3 days before MPM isolation. Total MPMs were harvested by washing the peritoneal cavity with PBS containing 30 mM of EDTA (8 mL per mouse), centrifuged and suspended in RPMI-1640 medium (Gibco/BRL life Technologies, Eggenstein, Germany) with 10% FBS (Hyclone, Logan, UT, USA), 100 U·mL^{-1} penicillin and 100 mg·mL^{-1} streptomycin. Non-adherent cells were removed by washing with medium 3 h after seeding. Before treatment, MPMs were cultured in 60 mm plates (1.2×10^6 cells per plate with 3 mL PRMI-1640 medium) and incubated overnight at 37°C in a 5% CO$_2$-humidified air.

Nitrite assay

Cell culture supernatant or plasma in animal experiments (100 μL) was collected and combined with 50 μL 1% sulfanilamide in 5% H$_3$PO$_4$ and 50 μL 0.1% N-(1-naphthyl) ethylenediamine dihydrochloride (Sigma) in water in a 96-well plate, followed by spectrophotometric measurement at 550 nm, using a microplate reader (MD, Sunnyvale, CA, USA). Nitrite concentration in the supernatant was determined by comparison with a sodium nitrite standard curve.

Determination of TNF-α

The TNF-α levels in cell medium or rat plasma were determined with an ELISA kit (Bioscience, San Diego, CA, USA) according to the manufacturer's instructions. The total amount of TNF-α in the cell medium was normalized to the total amount of protein in the viable cell pellets. Experiments were performed in duplicate.

Real-time quantitative PCR

Cells or kidney tissues (50–100 mg) were homogenized in TRIZOL (Invitrogen, Carlsbad, CA, USA) or prepared with a PARIS kit (Ambion, Austin, TX, USA) for extraction of RNA according to each manufacturer's protocol. Both reverse transcription and quantitative PCR were carried out using a two-step M-MLV Platinum SYBR Green qPCR SuperMix-UDG kit (Invitrogen, Carlsbad, CA, USA). Eppendorf Mastercycler ep realplex detection system (Eppendorf, Hamburg, Germany)

were used for q-PCR analysis. The primers of genes including iNOS, COX-2, TNF-α, IL-6, IL-1β, IL-12, TGF-β, MCP-1, CD68 and β-actin were synthesized from Invitrogen (Invitrogen, Shanghai, China). The primer sequences used were listed in Table S1. The amount of each gene was determined and normalized to the amount of β-actin.

Western immunoblot analysis

Either collected cells or homogenated kidney tissue samples were lysated. Thirty micrograms of lysates were separated by 10% SDS-PAGE and electrotransferred to a nitrocellulose membrane. Each membrane was pre-incubated for 1 h at room temperature in Tris-buffered saline, pH 7.6, containing 0.05% Tween 20 and 5% non-fat milk. Each nitrocellulose membrane was incubated with specific antibodies. Immunoreactive bands were then detected by incubating with secondary antibody conjugated with horseradish peroxidase and visualizing using enhanced chemiluminescence reagents (Bio-Rad, Hercules, CA, USA). The amounts of the proteins were analysed using Image J analysis software version 1.38e (NIH, Bethesda, MD, USA) and normalized to their respective control.

Assay of cellular NF-κB p-65 translocation

The cells were immunofluorescence-labelled according to the manufacturer's instruction using a Cellular NF-κB p65 Translocation Kit (Beyotime Biotech, Nantong, China) by the method described by Xu et al. (2008). P65 protein and nuclei, fluoresce as red and blue, respectively, were simultaneously viewed by fluorescence microscope (200×; Nikon, Tokyo, Japan) at an excitation wavelength of 350 nm for DAPI and 540 nm for cyanine 3 (Cy3). To create a two-colour image, the red and blue images were overlaid.

Animal experiments

SD rats were randomly divided into five groups with six rats in each group: (i) non-diabetic control rats (SD group); (ii) streptozotocin (STZ)-induced diabetic rats that received vehicle alone (DM group); (iii) STZ-induced diabetic rats that were treated p.o. with C66 (in 1% CMC-Na solution) at a dose of 0.2 mg·kg^{-1}·day^{-1} starting at day 7 after STZ injection for 6 weeks (DM + C66 0.2 mg·kg^{-1} group); (iv) DM + C66 1.0 mg·kg^{-1} group; and (v) DM + C66 5.0 mg·kg^{-1} group. The effective doses of C66 were based on the results from the cellular experiments.

Diabetes was induced in 5-week-old SD rats by a single i.v. injection of 60 mg·kg^{-1} STZ (Sigma) in citrate buffer (pH 4.5), as described previously (Yozai et al., 2005). Non-diabetic control rats received an injection of citrate buffer alone. C66 was dissolved in 1% CMCNa solution, and animals in the C66 treatment groups were treated with C66 (p.o.) 0.2, 1 or 5 mg·kg^{-1}·day^{-1}. The DM group received 1% CMC-Na solution alone in the same schedule as the C66 treatment groups. Body weights were checked weekly. Blood glucose was measured at day 7, 9, 16, 22, 40 and 49 after STZ induction with a glucometer. At day 49 after STZ induction, the rats were killed under ether anaesthesia, and then blood samples were taken from the right ventricle using a heparin-containing syringe with a needle. At the time of death, both kidneys were

removed and weighed. Serum TNF-α levels were detected by ELISA, and creatinine levels were determined by an automatic biochemical analyser.

Renal histopathology

Kidneys were fixed in 4% paraformaldehyde and embedded in paraffin. The paraffin sections (5 μm) were stained with haematoxylin and eosin (H&E). To estimate the extent of damage, the specimen was observed under a light microscope (400× amplification; Nikon).

Immunohistochemistry

After deparaffinization and rehydration, 5 μm kidney sections were treated with 3% H_2O_2 for 10 min and with 1% BSA in PBS for 30 min. Slides were incubated overnight at 4°C with anti-CD68 antibody (1:50) then incubated with fluorescein isothiocyanate (FITC)-labelled secondary antibody (Santa Cruz; 1:500) for 1 h at room temperature. Then the cell nuclei were stained with DAPI for 5 min, and the images were viewed by a fluorescence microscope (400×, amplification; Nikon).

PAS staining for glycogen and Sirius red staining for type IV collagen

Tissues were fixed in paraformaldehyde solution and embedded in paraffin. Paraffin sections (5 μm) of the renal tissues were stained with 0.5% periodic acid and Schiff solution (PAS) to evaluate the glycogen content, or were stained with 0.1% Sirius red F3B and 1.3% saturated aqueous solution of picric acid to evaluate the type IV collagen level. The stained sections then were viewed by fluorescence microscope (400×; Nikon).

Statistical analysis

The results are presented as means ± SEM. The statistical significance of differences between groups was obtained by means of ANOVA followed by Student's t-test of comparison.

$P < 0.05$ was considered as an indication of statistical significance. All experiments on cells were repeated at least three times.

Results

C66 reduced the production of TNF-α and NO in HG-stimulated MPMs

We first examined whether C66 could inhibit HG-induced increases in TNF-α and nitrite *in vitro*. MPMs were pretreated with C66 (5 μM) or vehicle for 2 h and then incubated with either LG (5.5 mM) or HG (25 mM) for 18 h. As shown in Figure 2, HG significantly increased TNF-α and nitrite production and C66 at 5 μM significantly inhibited the secretion of TNF-α and nitrite induced by HG ($P < 0.01$). Curcumin at 5 μM was used as a comparison control. As expected, C66 at the same concentration showed significantly stronger inhibition against HG-induced TNF-α expression when compared with the curcumin ($P < 0.05$). To examine whether high osmotic conditions play a role in HG-induced increase in cytokine gene expression, mannitol (25 mM) was used as a control. Figure 2 shows that treatment with mannitol did not change the TNF-α and nitrite profiles, indicating that HG stimulates cytokine expression via an inflammatory pathway. In addition, C66 itself did not increase the inflammatory response.

C66 significantly inhibited HG-induced IL-1β, TNF-α, IL-6, IL-12, COX-2 and iNOS mRNA transcription in MPMs

We next examined whether C66 could alter HG-induced inflammatory gene expression at the mRNA level. MPMs were pretreated with C66 or vehicle for 2 h, followed by LG or HG incubation for 3 h. Mannitol was used to eliminate the effect of high osmotic pressure and curcumin at 10 μM was utilized as a comparison. The results in Figure 3 show that HG
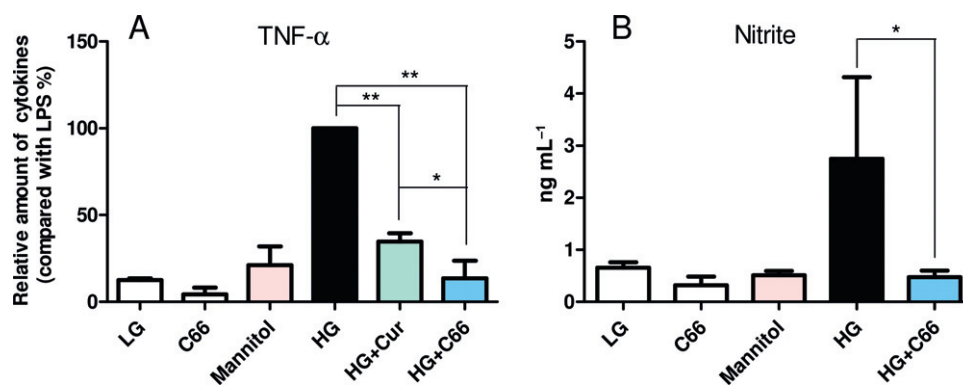

Figure 2

C66 inhibits HG-induced TNF-α and nitrite production. MPMs (1×10^6) were pretreated with Cur (curcumin, 5 μM) or C66 (5 μM) or vehicle (DMSO) for 2 h and then stimulated with HG (25 mM) for 18 h. Cells in LG group are cultured in PRMI-1640 medium containing 5.5 mM glucose. Cells in the C66 group only received 5 μM C66, and cells in the mannitol group were only treated with 25 mM mannitol. The levels of TNF-α (A) and nitrite (B) in medium were detected as described in Methods. Columns represent the mean ± SEM of three independent experiments performed in duplicate, and asterisks indicate significant inhibition (*$P < 0.05$, **$P < 0.01$).
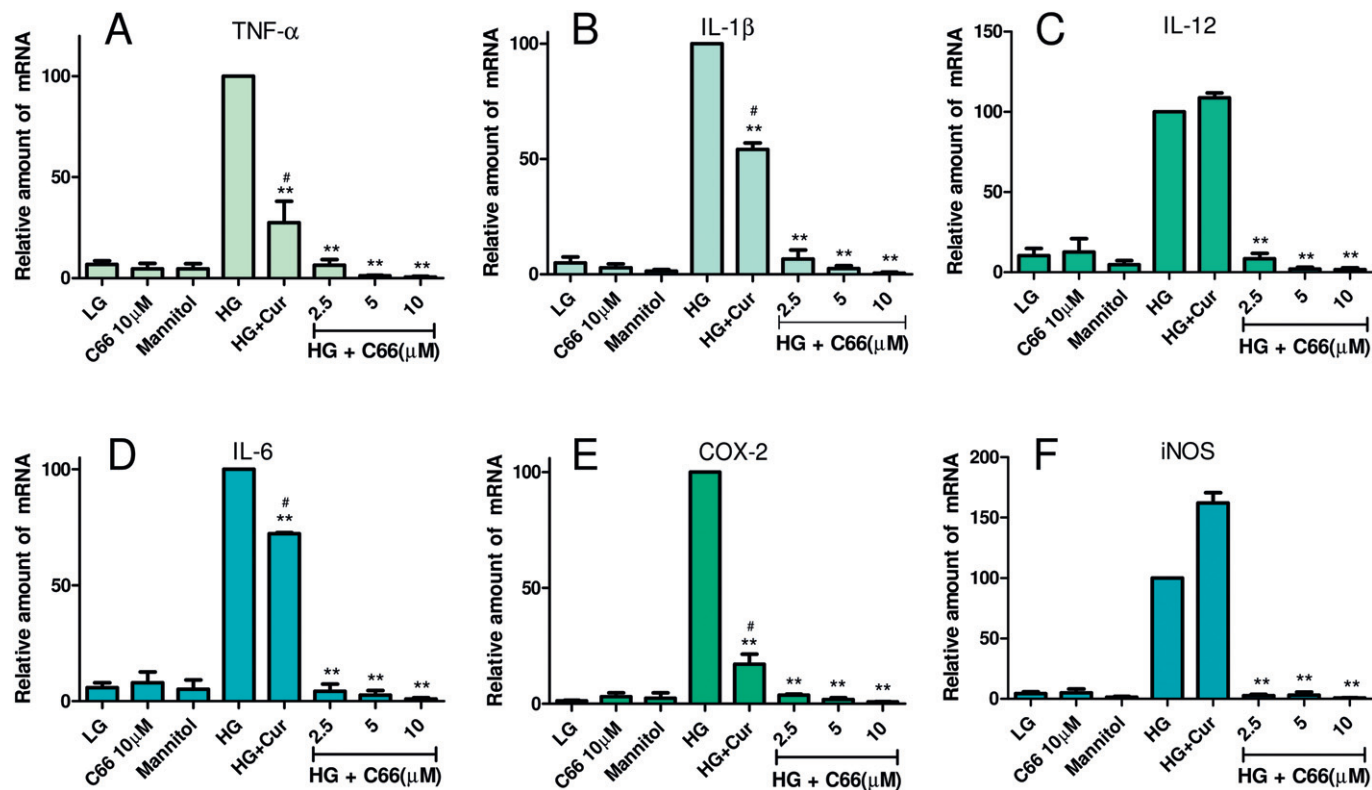
Figure 3
C66 inhibits HG-induced inflammatory mRNA expression in MPMs. MPMs (1×10^6) were pretreated with Cur (curcumin, 10 μM), C66 (2.5, 5 and 10 μM) or vehicle (DMSO, 3 μL) for 2 h and then stimulated with HG (25 mM) for 3 h. Cells in the LG group were cultured in PRMI-1640 medium containing 5.5 mM glucose. Cells in the C66 group only received 10 μM C66, and cells in the mannitol group were only treated with 25 mM mannitol. The mRNA levels of TNF-α (A), IL-1β (B), IL-12 (C), IL-6 (D), COX-2 (E) and iNOS (F) were detected by RT-qPCR as described in Methods. Columns represent the mean ± SEM of three independent experiments performed in duplicate, and asterisks indicate significant inhibition (*$P < 0.05$, **$P < 0.01$ vs. HG group; #$P < 0.05$ vs. C66 10 μM group).

induced a significant increase in the mRNA expression of pro-inflammatory cytokines, including TNF-α (A), IL-1β (B), IL-12 (C), IL-6 (D) and inducible enzymes such as inducible NOS (iNOS, D) and COX-2 (E), while C66 dose-dependently (2.5, 5 and 10 μM) decreased the HG-induced increase in mRNA expression of pro-inflammatory cytokines ($P < 0.01$). Compared with C66, curcumin only showed a moderate down-regulation in HG-induced mRNA expression ($P < 0.05$). C66 or mannitol alone did not alter the levels of expression of inflammatory genes. These data indicate that C66 is a potent inhibitor of HG-induced mRNA overexpression of inflammatory genes in MPMs.

C66 suppressed the HG-induced activation of JNK/NF-kB signalling in MPMs

Curcumin has been identified as an inhibitor of JNK/NF-κB-dependent inflammation (Hanai and Sugimoto, 2009). During the activation of NF-κB, phosphorylation and degradation of IκBα leads to the separation of IκBα from NF-κB p65 subunit and then releases the p65 for translocation from the cytoplasm to nuclei (Jeon *et al.*, 2010). As shown in Figure 4A, HG accelerated NF-κB p65 nuclear translocation (red point in blue nuclei), whereas in C66-pretreated cells, HG-induced

nuclear p65 decreased, suggesting that C66 inhibited p65 translocation. Western blot analysis also showed that C66 dose-dependently reduced the HG-induced increase nuclear p65 levels and slightly increased the HG-induced decrease in cytosolic p65 levels (Figure 4B). We next evaluated the effects of C66 on IκBα phosphorylation and degradation in MPMs. Figure 4C and D demonstrate that HG increased IκBα phosphorylation and degradation after 30 min of incubation, whereas pretreatment with C66 (2.5, 5 or 10 μM) dose-dependently reduced this HG-induced IκBα phosphorylation and degradation, respectively. JNK has been established as a key transcriptional regulator of inflammatory cytokines. Our results (Figure 4E) show that C66 (2.5, 5 or 10 μM) also dose-dependently inhibited HG-induced JNK phosphorylation in macrophages, suggesting that the anti-inflammatory activity of C66 is associated with its negative effects on JNK/NF-κB activation.

C66 significantly inhibited the raised plasma TNF-α level and renal inflammatory gene expression in type I diabetic rats

Inflammation plays an important role in the pathophysiology of diabetic renal complications (Donath *et al.*, 2010; Tang
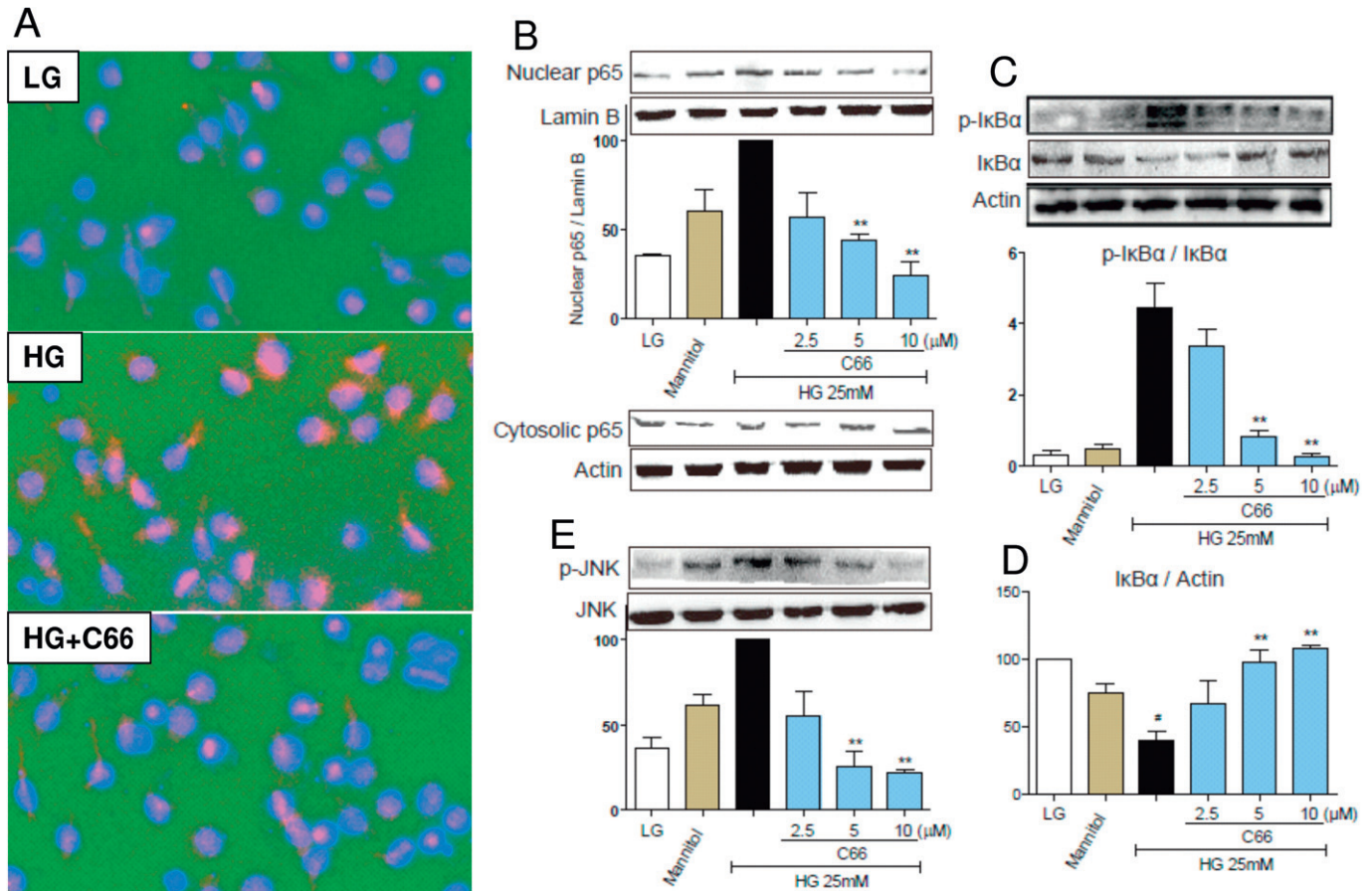
Figure 4

C66 inhibits HG-induced JNK/NF-κB activation in MPMs. MPMs were pretreated with vehicle (DMSO) or C66 (2.5, 5 or 10 μM) for 2 h and then stimulated with HG (25 mM) for 30 min. Cells in the LG group were cultured in PRMI-1640 medium containing 5.5 mM glucose. Cells in the mannitol group were only treated with 25 mM mannitol. (A) Immunofluorescence-labelled staining for NF-κB p65 translocation was performed as described in Methods. Similar results were observed in three independent experiments. (B) The nuclear proteins and cytoplasmic proteins were isolated as described in Methods. The nuclear p65 and cytosolic p65 were detected by Western blot using Lamin B and actin as loading control respectively. (C–E) The levels of p-IκBα, IκBα and p-JNK were examined using specific antibodies with actin and JNK as the loading control, respectively. The column figures in (B)–(E) show the normalized optical density as percentage of HG or LG group. Columns represent the mean ± SEM of three independent experiments (*$P < 0.05$, **$P < 0.01$, vs. HG group; #$P < 0.01$ vs. C66 LG group).

et al., 2010; Zong et al., 2010). Our in vitro results demonstrated the inhibitory effects of C66 on HG-induced inflammatory gene expression in MPMs. In order to determine whether C66 affects HG-induced inflammatory process in vivo, we set up STZ-induced type I diabetic rat models treated with C66 (p.o., 0.2, 1 and 5 mg·kg^{-1}·day^{-1}) or vehicle for 6 weeks. TNF-α is one of the most important pro-inflammatory factors in diabetic nephropathy. Figure 5A shows that circulating TNF-α levels were significantly increased in diabetic rats, while administration of C66 at 0.2, 1 and 5 mg·kg^{-1}·day^{-1} dose-dependently reduced the plasma level of TNF-α compared with that in the DM group. Furthermore, inflammatory genes, such as TNF-α, COX-2 and iNOS, were also overexpressed in diabetic rat kidneys (6.0-, 4.1- and 3.8-fold, respectively), and C66 administration significantly decreased the overexpression of these genes in a dose-dependent manner (Figure 5B and D). However, our results showed that C66 at 5 mg·kg^{-1}·day^{-1} did not affect the renal COX-2 mRNA expression.

TGF-β and MCP-1 are involved in renal inflammation and fibrosis in diabetic models (Shi et al., 2010; Jiang et al., 2011). Figure 5E and F showed that renal TGF-β and MCP-1 mRNA expression were significantly increased in diabetic rats as compared with those in control rats ($P < 0.01$). This up-regulation of TGF-β and MCP-1 mRNA in diabetic kidney was significantly reduced by treatment with C66 in a dose-dependent manner. These data suggest that C66 is able to inhibit inflammatory gene expression in diabetic kidneys.

C66 inhibited NF-κB activation in the diabetic kidney

To confirm that C66-induced down-regulation of in vivo inflammatory genes is also associated with the NF-κB pathway, Western blot analysis was performed using kidney tissues from C66-treated or untreated diabetic rats. As shown in Figure 6, administration of C66 (5 mg·kg^{-1}) for 6 weeks, similar to the in vitro results, markedly inhibited diabetes-induced renal IKKα expression ($P < 0.01$) and IκBα (Ser$^{32/36}$)
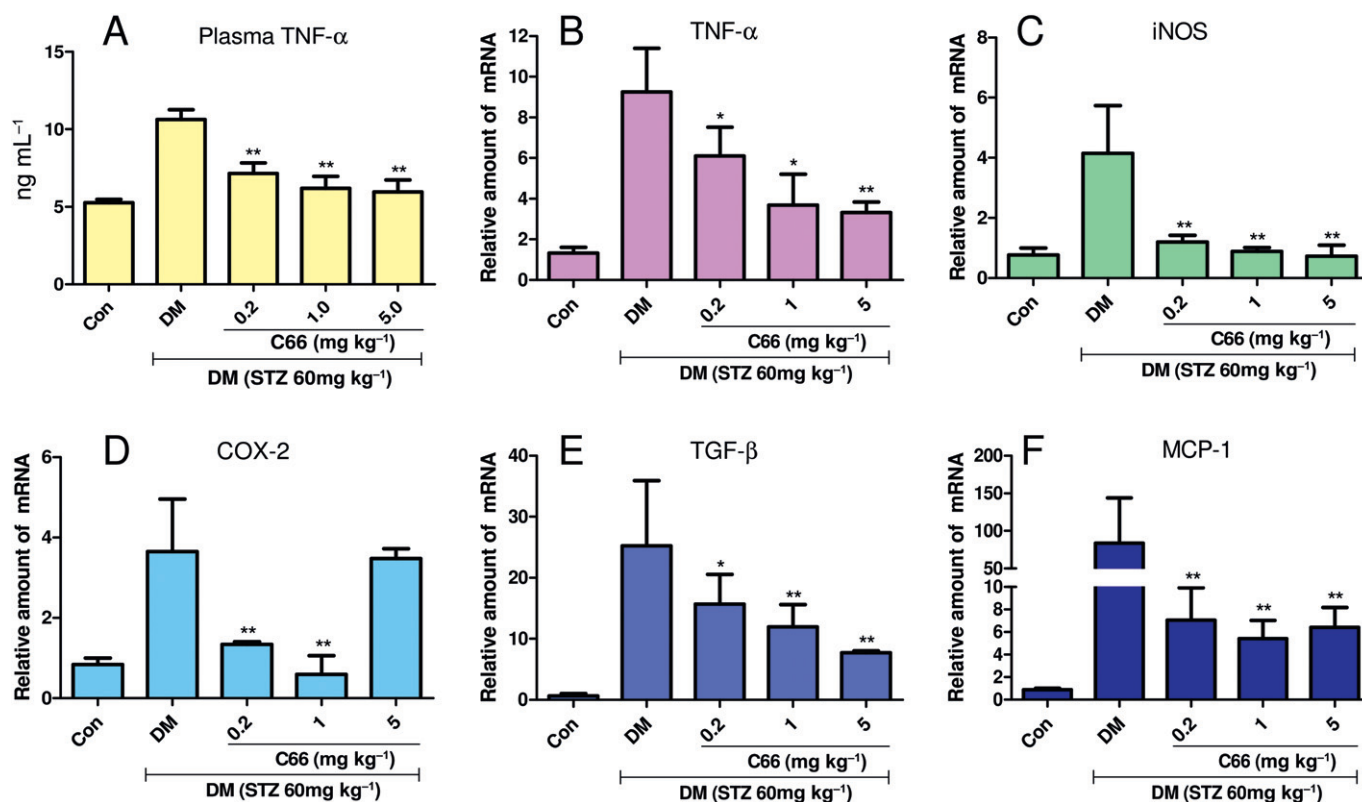
Figure 5

Effects of C66 on serum TNF-α level (A), renal TNF-α (B), renal iNOS (C), renal COX-2 (D), renal TGF-β (E) and renal MCP-1 (F) in diabetic rats at the time of death. The TNF-α level was determined by ELISA, while renal mRNA expression of TNF-α, iNOS, COX-2, TGF-β and MCP-1 were estimated by the RT-qPCR. The mRNA expression of five genes was normalized to β-actin mRNA content. Columns show mean ± SEM from five rats in each group (Con, control group; *$P < 0.05$, **$P < 0.01$, vs. the DM group).

phosphorylation ($P < 0.05$) when compared with those in the control (DM) group. C66 also had an inhibitory effect on diabetes-induced renal p65 phosphorylation (Ser[536]) that contributes to its translocation from the cytoplasm to nuclei ($P < 0.01$).

C66 reduced interstitial macrophage infiltration in the diabetic kidney

Besides the inhibition on inflammatory response by C66 in macrophages, we also investigated the effect of C66 on macrophage infiltration in the diabetic kidneys. Immunohistochemistry staining for CD68 was performed using kidney tissues from C66-treated or untreated diabetic rats to observe focal interstitial macrophage infiltration. As shown in Figure 7A–E, the diabetic rats had a significant increase in CD68-positive macrophages in interstitial areas, while macrophages were not found in the control kidneys. C66 dose-dependently reduced renal CD68+ macrophage infiltration in the diabetic rats ($P < 0.01$). This result was also confirmed by Western blot and RT-qPCR analysis. Figure 7F and G demonstrate a significant attenuation of renal CD68 expression at the levels of both protein and mRNA after administration of C66 at 5 mg·kg^{-1}·day^{-1} in diabetic rats.

C66 administration did not affect blood glucose levels and body weight in diabetic rats

Blood glucose levels of the DM group and C66 treatment groups were much higher than that of the control group, whereas there were no significant differences in blood glucose levels between the DM group and C66 treatment groups (Figure 8A). Mean values of body weight of the DM group and C66 treatment groups were lower than that of the control group; similarly, there was no significant difference in body weight between the DM group and C66 treatment groups (Figure 8B). These data suggest that C66 does not attenuate this diabetic symptom in rats, and its inhibition of the inflammatory response in diabetic kidney does not result from a lowering of the glucose level.

C66 administration reduced serum creatinine and kidney/body weight ratio in diabetic rats

The anti-inflammatory activity of C66 in diabetic kidney may contribute to its protection of diabetic renal complications. Serum creatinine and kidney/body weight ratio are two hallmarks of renal injury and fibrosis (Barutta et al., 2010). Seven weeks after STZ induction of diabetes, the mean serum creatinine level of the DM group was higher than that of the
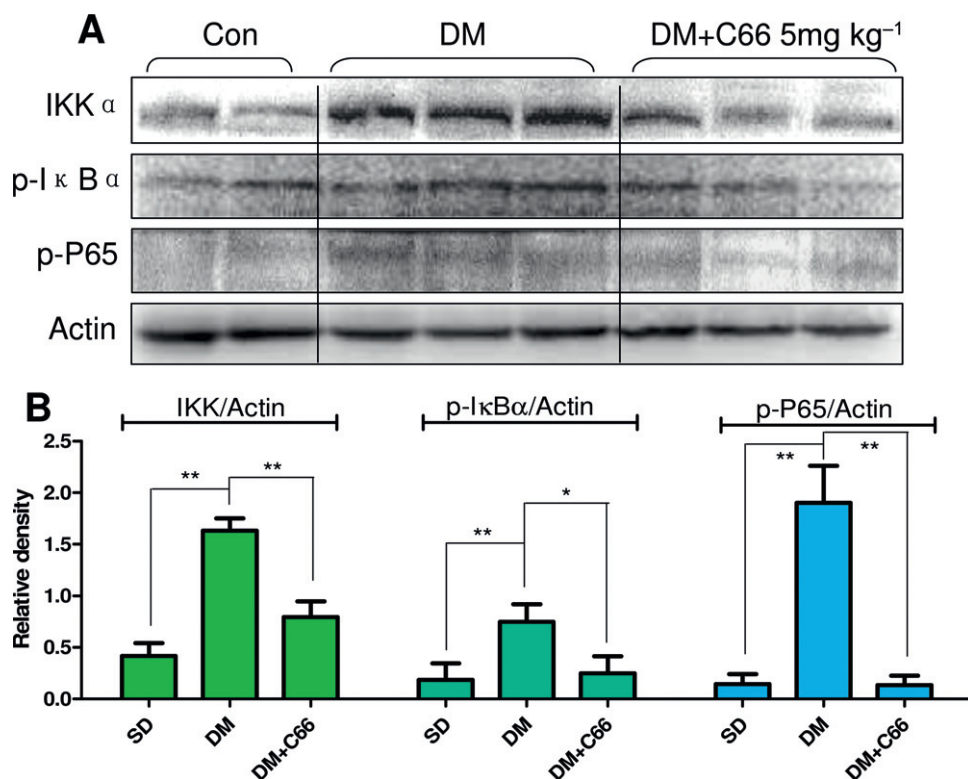
Figure 6

Effects of C66 (5 mg·kg^{-1}·day^{-1}) on renal NF-κB activation in diabetic rats. After the diabetic rats were killed, the rat kidney tissues in control group (Con), DM group and DM + C66 5 mg·kg^{-1} group were collected and homogenized to detect IKKα, p-IκBα and p-p65 by Western blot. Actin was used as a loading control. The columns show the normalized optical density of respective protein and represent the mean ± SEM of each group (two rats in SD group, three rats in DM group, three rats in DM + C66 5 mg·kg^{-1} group) (*$P < 0.05$, **$P < 0.01$).

control group ($P < 0.01$); however, this diabetes-induced increase in serum creatinine was significantly attenuated in the C66 treated groups compared with the DM group ($P < 0.05$, Figure 8C); C66 administration inhibited serum creatinine level in DM rats in a dose-dependent manner (1 mg·kg^{-1}·day^{-1}, $P < 0.05$; 5 mg·kg^{-1}·day^{-1}, $P < 0.01$). As shown in Figure 8D, kidney weight in relation to body weight was significantly increased in the DM group ($P < 0.05$) compared with that of the control group, whereas a decrease was observed in C66 treated groups compared with DM group, especially in the C66 5 mg·kg^{-1}·day^{-1} group ($P < 0.05$).

C66 treatment improved histological abnormalities and fibrosis of diabetic kidney

All upstream anti-inflammatory actions of C66 ultimately lead to an improvement in the renal histolopathological abnormalities of diabetic rats. We examined the renal glycogen and type IV collagen collection and histopathology in 6 week C66-treated and untreated diabetic rats, using PAS, Sirius red and H&E staining, respectively. PAS staining (Figure 9A) demonstrated that C66 induced a dose-dependent inhibition of diabetes-induced glycogen collection (purple plaques) in rat kidney. Sirius red staining for type IV collagen (red plaques) revealed a significant increase in renal fibrosis in type I diabetic rats but not in C66-treated diabetic rats (Figure 9B). The H&E staining, determined by use of an optical microscope

(Figure 9C), revealed the glomerulus with glomerulosclerosis and expansion, diminution of capillary lumen, predominance of dense hyaline matrix and peripheral capillaries of thick stiff wall in the diabetic rats, whereas C66 treatment markedly ameliorated these diabetes-induced histopathological alterations. In addition, inflammatory cell infiltration and diffuse mesangial matrix expansion were also observed in the DM group, whereas these two pathological alterations were decreased in the C66-treated DM group. These results indicate that administration of C66 significantly improves the histological abnormalities and fibrosis of diabetic kidney.

Discussion and conclusions

Macrophages have been implicated in the development of chronic inflammation-mediated kidney lesions in diabetic rats (Tesch, 2010). During chronic inflammatory responses in diabetic subjects, macrophages infiltrate and accumulate in the kidney (Tesch, 2010). Recent data have also shown that HG treatment activates monocytes and induces an increase in gene expression of TNF-α, IL-1β and MCP-1 in human monocyte-like cells (Shanmugam et al., 2003). Our results also demonstrated that the HG-stimulated increase in cytokine mRNA transcription was not elicited by mannitol-induced high osmotic pressure, indicating that HG induces
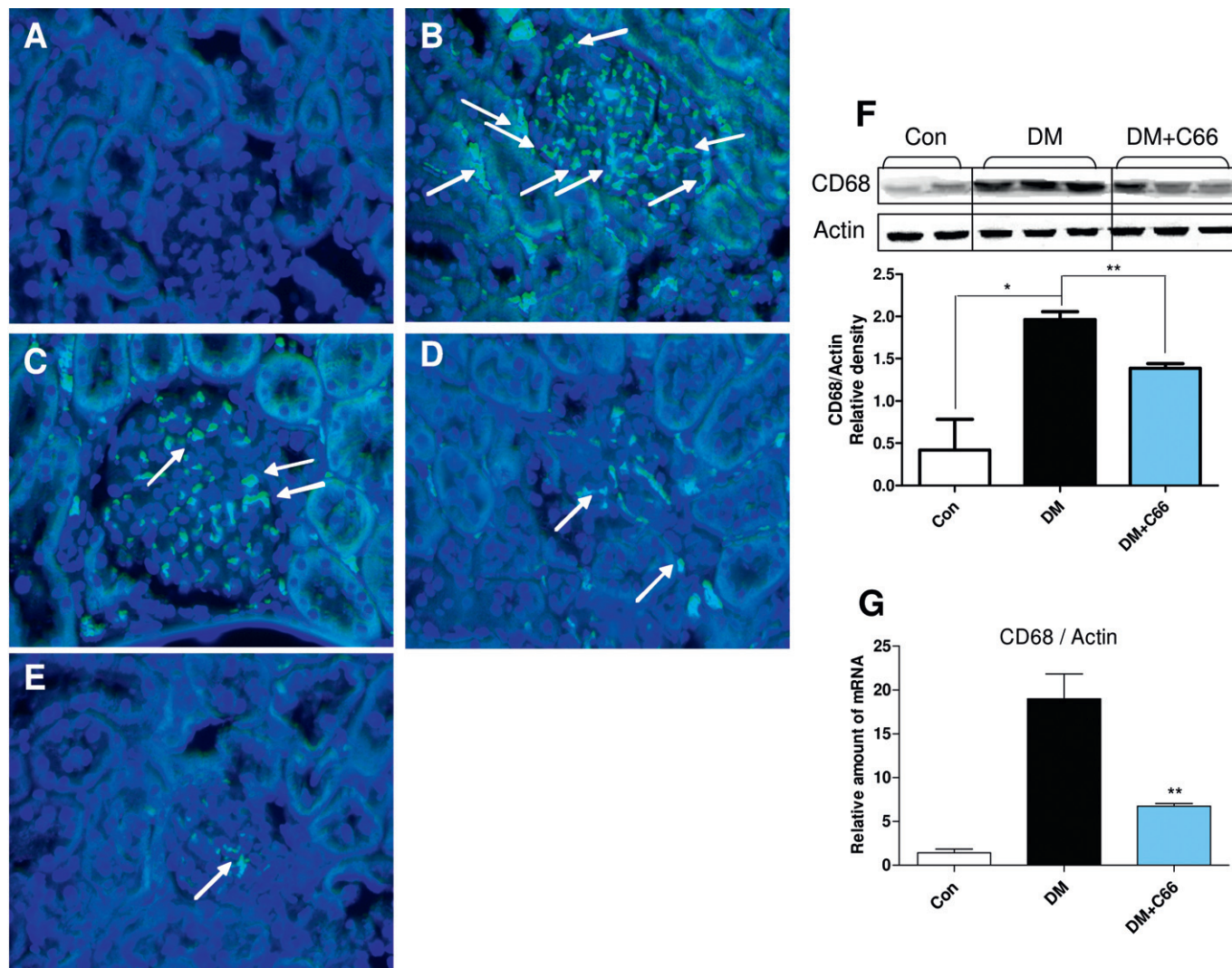
Figure 7
C66 inhibits renal macrophage infiltration in diabetic rats. Rats were treated, and kidney samples were prepared as described in Methods. (A–E) Macrophage infiltration was evaluated using anti-CD68 antibodies. (A) Control group. (B) DM group. (C) DM + C66 0.2 mg·kg^{-1} group. (D) DM + C66 1.0 mg·kg^{-1} group. (E) DM + C66 5.0 mg·kg^{-1} group. Arrows indicate stained interstitial inflammatory cells. Magnification, ×200. A representative animal out of five studied in each group is shown. (F–G) The rat kidney tissues from control group (Con), diabetes group (DM) and DM + C66 5 mg·kg^{-1} group were collected and homogenated. The protein level of CD68 was detected by Western blot. Actin was used as a loading control. The column figures show the normalized optical density of CD68/Actin (F). The mRNA expression of CD68 was estimated by the RT-qPCR and normalized to β-actin mRNA content (G). Bar graph shows mean ± SEM in each group (*$P < 0.05$, **$P < 0.01$).

inflammation via a classic transcriptional or post-transcriptional mechanism. Yonemoto *et al*. (2006) reported that macrophages were present in the kidneys of patients with diabetic nephropathy in addition to mesangial matrix expansion and interstitial fibrosis. As a result, recruited macrophages increase the expression of leucocyte adhesion molecules and release inflammatory cytokines such as IL-1β, IL-6, IL-12, IL-18, TNF-α, IFN-γ and MCP-1 (Hirata *et al*., 1998; Wen *et al*., 2006) via an NF-κB-dependent mechanism, contributing to an increase in albuminuria and renal fibrosis.

Curcumin has been identified as an inhibitor of NF-κB-dependent inflammation *in vitro* and *in vivo*, and also reduces HG-induced inflammatory gene expression by modulating the NF-κB pathway (Hanai and Sugimoto, 2009; Panicker and

Kartha, 2010). Our previous study have discovered a new compound C66 exhibiting a higher anti-inflammatory activity than the parent curcumin in *in vitro* LPS-challenged macrophages (Liang *et al*., 2009b). In the present study, we firstly demonstrated that C66 is a stronger anti-inflammatory compound than curcumin in HG-stimulated MPMs (Figures 2 and 3).

Amongst the intracellular signalling systems involved in the regulation of inflammatory and immune responses, NF-κB is of special interest. The upstream IKKα interacts with IκB-α and specifically phosphorylates IκBα on serines 32 and 36 and induces degradation (Adli *et al*., 2010). The dissociation of IκB from the inactive cytoplasmic complex leads to the translocation of the active subunit NF-κB p65 from the
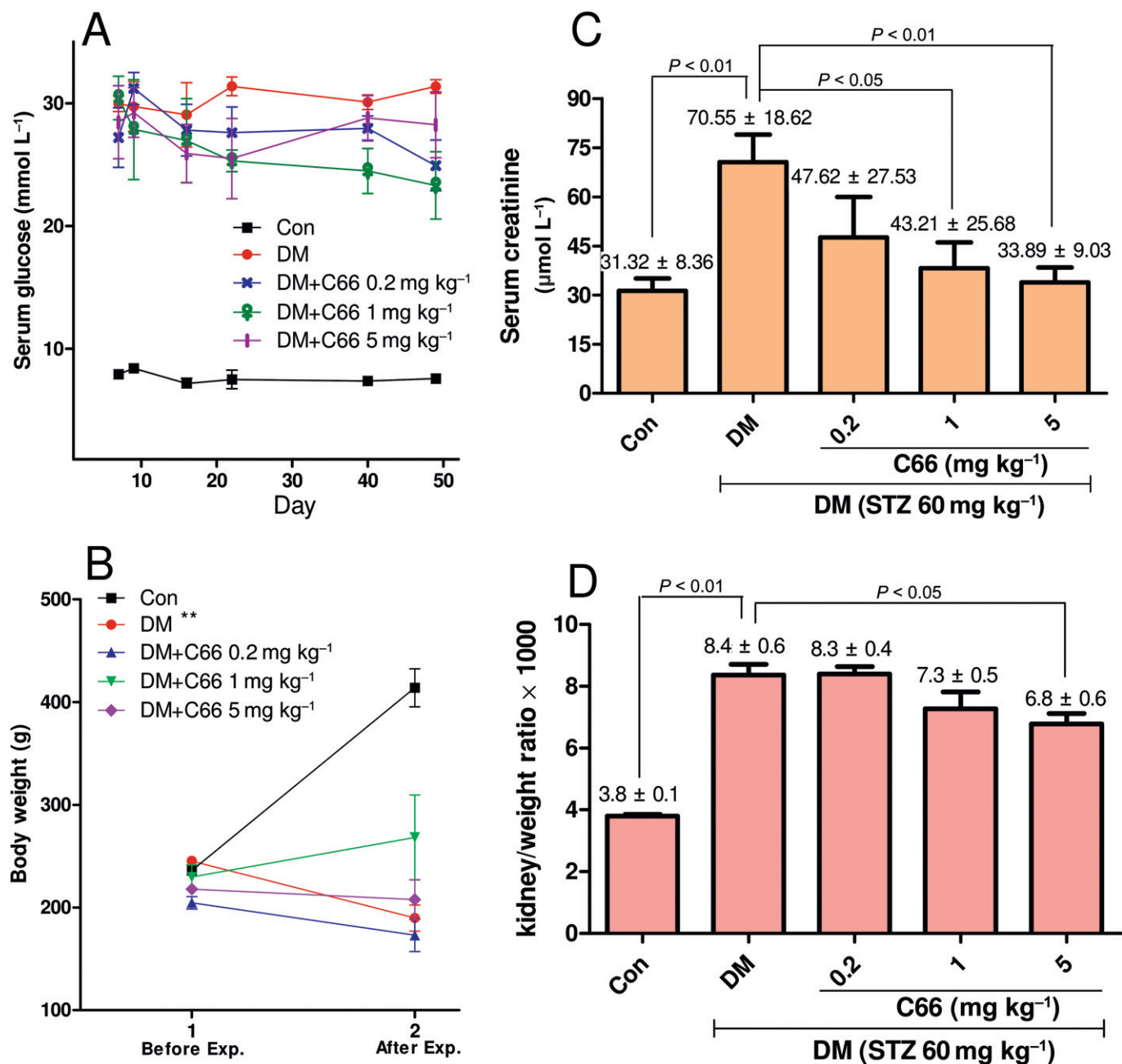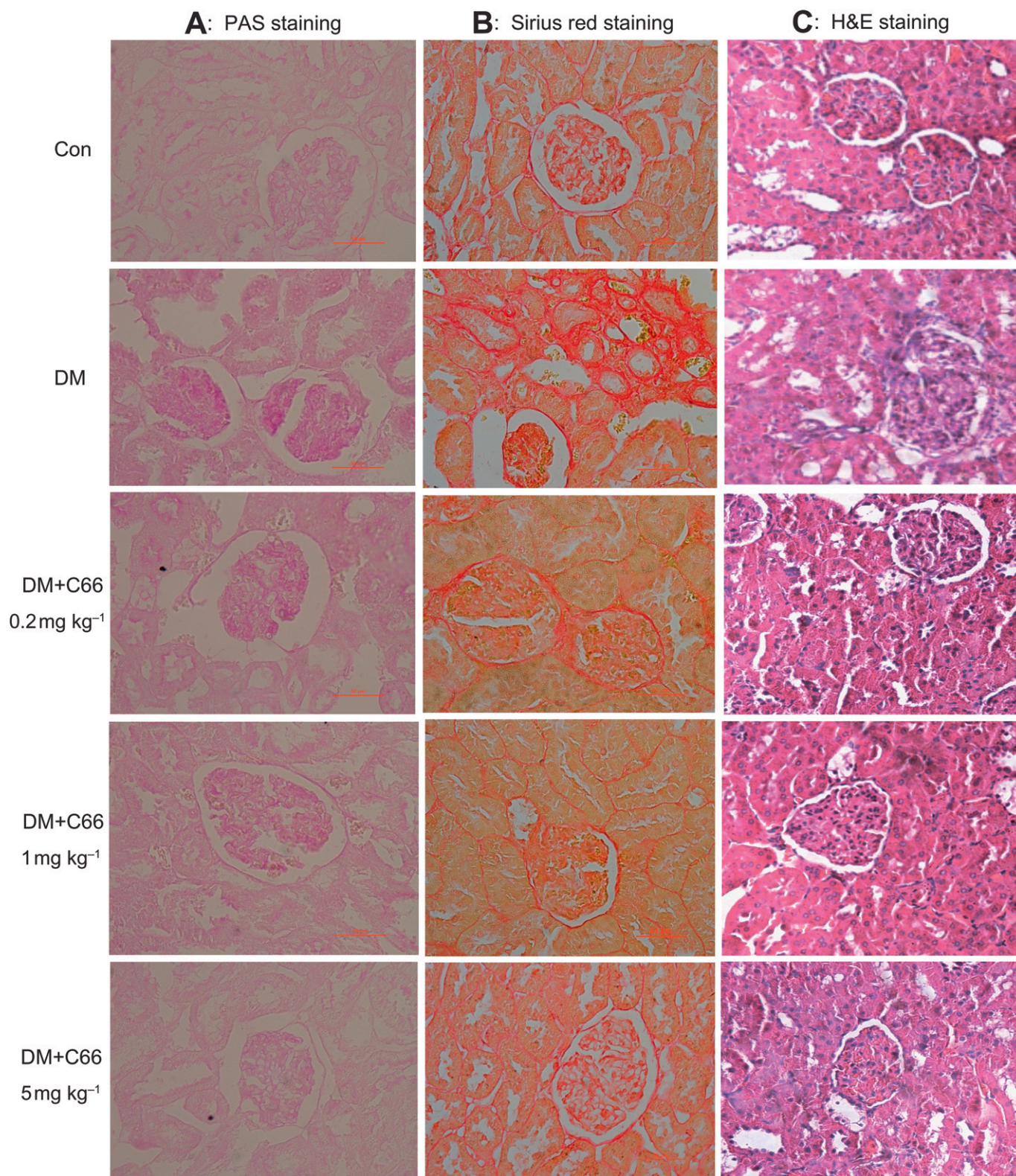
Figure 8

C66 affects the metabolic profiles of diabetic rats: serum glucose (A), body weight (B), serum creatinine (C) and kidney/body weight ratio (D). The serum glucose levels were detected at indicated times. Body weight of rats was detected at the beginning of STZ administration and the time of death, respectively. Serum creatinine and kidney/body weight ratio were detected at the time of death. The determinations of these four indexes are as described in Methods. Data are means ± SEM (Con, control group; *$P < 0.05$, **$P < 0.01$).

cytosolic to the nuclear fractions, this then binds to the DNA sites and triggers gene expression. Lee *et al.* (2008) found that high glucose (25 mM) increased NF-κB transcription activity by raising IκB phosphorylation and the nuclear p65 level in primary cultured HUVECs. In MPMs, HG stimulation also causes a significant activation of NF-κB signal (Wen *et al.*, 2006). Our results in Figure 4 (*in vitro*) and Figure 6 (*in vivo*) suggest that C66 negatively affects a series of procedures in HG-induced NF-κB activation, including IKK phosphoryla-

tion, IκBα phosphorylation and degradation and p65 nuclear translocation, indicating that the anti-inflammatory actions of C66 are associated with transcriptional suppression of the NF-κB pathway. In addition to NF-κB, JNK is activated by high glucose (Stan *et al.*, 2011). JNK is also an important player in inflammation and regulates the transcription of a number of inflammatory cytokines (Bage *et al.*, 2010). Herein, we further showed that C66-induced NF-κB inactivation was accompanied by effects on JNK dephosphorylation

A: PAS staining   **B**: Sirius red staining   **C**: H&E staining

Con

DM

DM+C66
0.2 mg kg⁻¹

DM+C66
1 mg kg⁻¹

DM+C66
5 mg kg⁻¹

Figure 9

C66 administration significantly improved histological abnormalities and fibrosis of diabetic kidney. (A) Representative figures of PAS staining (400×) for glycogen on renal tissue (seventh week). (B) Representative figures of Sirius red staining (400×) for type IV collagen on renal tissue (seventh week). (C) Renal histopathological analysis was performed using H&E staining as described in Methods (200×). Results from a representative animal out of five studied in each group are shown.

(Figure 4E), suggesting that C66 may target JNK kinase and inhibit NF-κB activation. However, it is unclear whether the anti-inflammatory effects of C66 are dependent on JNK/NF-κB. In addition, although curcumin down-regulates the JNK/NF-κB pathway, its molecular target for direct binding is still unknown. Our studies indicated that C66 has the same anti-inflammatory mechanism as curcumin. However, continued research is needed to examine the underlying molecular target of C66 at the transcriptional level.

Diabetic complications are mainly caused by a whole-body condition of high glucose (hyperglycaemia). Inflammatory biomarkers are associated with the development and progression of diabetic nephropathy. Activation of renal NF-κB has also been described in proteinuric kidney diseases and is associated with the overexpression of pro-inflammatory factors (Mezzano et al., 2001). Studies on the effects of mycophenolate mofetil (Utimura et al., 2003), infliximab (Moriwaki et al., 2007) and methotrexate (Yozai et al., 2005) have suggested that their inhibitory actions on inflammatory factors and NF-κB activation may be therapeutic in the treatment of DN. Also there is increasing evidence that an anti-inflammatory action is beneficial for the prevention of renal injury in diabetic animals (He et al., 2009; Decleves and Sharma, 2010).

C66 treatment did not decrease the STZ-caused hyperglycaemia (Figure 8A). However, we found that C66 treatment significantly down-regulated a part of physiological and pathological indexes of diabetic nephropathy, such as circulating creatinine (Figure 8C) and kidney/body weight ratio (Figure 8D), in a dose-dependent manner. Histopathological staining demonstrated that C66 treatment significantly improved diabetes-caused renal injury and dose-dependently reduced the collections of renal glycogen and type IV collagen (Figure 9). Suppression of creatinine and type IV collagen might be involved in the renoprotective effects of C66 in the late stage of diabetic nephropathy.

These in vivo results, combined with those obtained in vitro, suggest that the preventative action of C66 on diabetic renal injury should be ascribed to its anti-inflammatory effects. C66 administration induced a significant down-regulation of plasma and renal pro-inflammatory proteins (Figure 5), indicating anti-inflammatory effects of C66 in the circulation and local kidney. The expressions of TGF-β and MCP-1 are partly controlled by the transcriptional NF-κB pathway (Jiang et al., 2011). We showed that C66 also dose-dependently reduced TGF-β and MCP-1 gene expressions in diabetic rat kidneys (Figure 5E and F). As discussed above, we noted that C66 treatment markedly suppressed NF-κB activation in the diabetic kidney (Figure 6). Together, these findings support the hypothesis that C66 inhibits the pro-inflammatory mediators at the transcriptional level and subsequently attenuates the inflammatory process in the diabetic kidney.

Macrophages are important immune cells, and their accumulation contributes to the development of renal injury and sclerosis. We further observed that the systemic administration of C66 in diabetic rats decreased the tubulointerstitial infiltration of macrophages (Figure 7). C66 also significantly reduced the diabetes-induced CD68 expression (Figure 7G). However, the degree of CD68 reduction by C66 is similar to that in the renal inflammatory cytokines (Figure 5). These data demonstrate that C66 treatment may attenuate the inflammatory cytokine expression in the whole kidney tissue, including a variety of renal cell types. The H&E staining results (Figure 9) further confirmed that C66 treatment reduced renal infiltration of leucocytes such as macrophages. MCP-1 is the best-described chemokine in human and experimental diabetic nephropathy; it contributes to the macrophage accumulation in diabetic kidney and is useful for monitoring kidney macrophage accumulation in diabetic nephropathy (Chow et al., 2006). In addition, the production of pro-inflammatory cytokines, such as IL-1β or TNF-α, also stimulates the increase in cell adhesion molecule expression. Our data demonstrate that C66 inhibits the expression of MCP-1 and TNF-α in diabetic kidney, suggesting a possible mechanism for the suppression of macrophage infiltration. Together, our data clearly show that the attenuation of the inflammatory factors by C66 was accompanied by a reduction of macrophage accumulation in diabetic kidney. Research using other renal cells will be needed to reveal the underlying mechanism by which C66 decreases the macrophage accumulation in diabetic kidney.

The parent compound, curcumin, has also been reported to protect the kidney from DN. Two independent groups found that chronic oral administration of curcumin (50 or 15–30 mg·kg^{-1}·day^{-1}, respectively) significantly ameliorated renal dysfunction in diabetic rats (Sharma et al., 2006; Tikoo et al., 2008). Chiu et al. (2009) demonstrated that curcumin (150 mg·kg^{-1}·day^{-1}, i.p., for 4 weeks) is beneficial in preventing the development of DN by inhibiting p300 and NF-κB. Although several studies showed curcumin is able to protect from diabetic renal injury, the dose of curcumin is relatively high, probably due to its poor bioavailability. More recently, however, a study in diabetic mice showed that administration of curcumin (5000–7500 ppm in diet, probably equal to 200–300 mg·kg^{-1}·day^{-1}) failed to attenuate DN (Ma et al., 2010). In our previous study we demonstrated the significantly improved pharmacokinetic profiles of the newly designed mono-carbonyl analogues of curcumin, including C66 (Liang et al., 2009a). In addition to improved pharmacokinetics, C66 showed a marked increase in anti-inflammatory ability, compared to curcumin. In keeping with such studies, the in vivo doses of C66 we used were 50–200-fold lower than those of curcumin. As expected, we found that C66 exhibited renal protective effects in vivo even at a low dose (0.2, 1 or 5 mg·kg^{-1}·day^{-1}).

In conclusion, our data demonstrate that a novel curcumin derivative, C66, is able to reduce the HG-induced inflammatory response, which was accompanied by inhibitory effects on JNK/NF-κB activation. Furthermore, the attenuation of the inflammatory process by C66 administration (even at a dose as low as 0.2 mg·kg^{-1}·day^{-1}) contributes to its renal protective effects in the diabetic rat. These results suggest that the novel compound C66 is a potential agent for the treatment of diabetic nephropathy via an anti-inflammatory mechanism and furthermore could be beneficial for the therapy of other chronic inflammatory diseases.

Acknowledgements

Conflicts of interest

The authors declare no competing financial interest.

References

Adli M, Merkhofer E, Cogswell P, Baldwin AS (2010). IKKalpha and IKKbeta each function to regulate NF-kappaB activation in the TNF-induced/canonical pathway. PLoS ONE 5: e9428.

Anand P, Kunnumakkara AB, Newman RA, Aggarwal BB (2007). Bioavailability of curcumin: problems and promises. Mol Pharm 4: 807–818.

Bage T, Lindberg J, Lundeberg J, Modeer T, Yucel-Lindberg T (2010). Signal pathways JNK and NF-κB, identified by global gene expression profiling, are involved in regulation of TNF-α-induced mPGES-1 and COX-2 expression in gingival fibrablasts. BMC Genomics 11: 241.

Barutta F, Corbelli A, Mastrocola R, Gambino R, Di Marzo V, Pinach S et al. (2010). Cannabinoid receptor 1 blockade ameliorates albuminuria in experimental diabetic nephropathy. Diabetes 59: 1046–1054.

Brevetti G, Giugliano G, Brevetti L, Hiatt WR (2010). Inflammation in peripheral artery disease. Circulation 122: 1862–1875.

Chiu J, Khan ZA, Farhangkhoee H, Chakrabarti S (2009). Curcumin prevents diabetes-associated abnormalities in the kidneys by inhibiting p300 and nuclear factor-kappaB. Nutrition 25: 964–972.

Chow FY, Nikolic-Paterson DJ, Ozols E, Atkins RC, Rollin BJ, Tesch GH (2006). Monocyte chemoattractant protein-1 promotes the development of diabetic renal injury in streptozotocin-treated mice. Kidney Int 69: 73–80.

Decleves AE, Sharma K (2010). New pharmacological treatments for improving renal outcomes in diabetes. Nat Rev Nephrol 6: 371–380.

Donath MY, Boni-Schnetzler M, Ellingsgaard H, Halban PA, Ehses JA (2010). Cytokine production by islets in health and diabetes: cellular origin, regulation and function. Trends Endocrinol Metab 21: 261–267.

Epstein J, Sanderson IR, Macdonald TT (2010). Curcumin as a therapeutic agent: the evidence from in vitro, animal and human studies. Br J Nutr 103: 1545–1557.

Garcea G, Jones DJ, Singh R, Dennison AR, Farmer PB, Sharma RA et al. (2004). Detection of curcumin and its metabolites in hepatic tissue and portal blood of patients following oral administration. Br J Cancer 90: 1011–1015.

Goldberg RB (2009). Cytokine and cytokine-like inflammation markers, endothelial dysfunction, and imbalanced coagulation in development of diabetes and its complications. J Clin Endocrinol Metab 94: 3171–3182.

Hanai H, Sugimoto K (2009). Curcumin has bright prospects for the treatment of inflammatory bowel disease. Curr Pharm Des 15: 2087–2094.

He LJ, Liang M, Hou FF, Guo ZJ, Xie D, Zhang X (2009). Ethanol extraction of Picrorhiza scrophulariiflora prevents renal injury in experimental diabetes via anti-inflammation action. J Endocrinol 200: 347–355.

Hirata K, Shikata K, Matsuda M, Akiyama K, Sugimoto H, Kushiro M et al. (1998). Increased expression of selectins in kidneys of patients with diabetic nephropathy. Diabetologia 41: 185–192.

Jeon KI, Xu X, Aizawa T, Lim JH, Jono H, Kwon DS et al. (2010). Vinpocetine inhibits NF-kappaB-dependent inflammation via an IKK-dependent but PDE-independent mechanism. Proc Natl Acad Sci U S A 107: 9795–9800.

Jiang Q, Liu P, Wu X, Liu W, Shen X, Lan T et al. (2011). Berberine attenuates lipopolysaccharide-induced extracelluar matrix accumulation and inflammation in rat mesangial cells: involvement of NF-kappaB signaling pathway. Mol Cell Endocrinol 331: 34–40.

Kaul K, Hodgkinson A, Tarr JM, Kohner EM, Chibber R (2010). Is inflammation a common retinal-renal-nerve pathogenic link in diabetes? Curr Diabetes Rev 6: 294–303.

Kopf M, Bachmann MF, Marsland BJ (2010). Averting inflammation by targeting the cytokine environment. Nat Rev Drug Discov 9: 703–718.

Kwong C, Gilman-Sachs A, Beaman K (2011). Tumor-associated a2 vacuolar ATPase acts as a key mediator of cancer-related inflammation by inducing pro-tumorigenic properties in monocytes. J Immunol 186: 1781–1789.

Lee YJ, Kang DG, Kim JS, Lee HS (2008). Effect of Buddleja officinalis on high-glucose-induced vascular inflammation in human umbilical vein endothelial cells. Exp Biol Med (Maywood) 233: 694–700.

Liang G, Li X, Chen L, Yang S, Wu X, Studer E et al. (2008). Synthesis and anti-inflammatory activities of mono-carbonyl analogues of curcumin. Bioorg Med Chem Lett 18: 1525–1529.

Liang G, Shao L, Wang Y, Zhao C, Chu Y, Xiao J et al. (2009a). Exploration and synthesis of curcumin analogues with improved structural stability both in vitro and in vivo as cytotoxic agents. Bioorg Med Chem 17: 2623–2631.

Liang G, Zhou H, Wang Y, Gurley EC, Feng B, Chen L et al. (2009b). Inhibition of LPS-induced production of inflammatory factors in the macrophages by mono-carbonyl analogues of curcumin. J Cell Mol Med 13: 3370–3379.

Ma J, Phillips L, Wang Y, Dai T, LaPage J, Natarajan R et al. (2010). Curcumin activates the p38MPAK-HSP25 pathway in vitro but fails to attenuate diabetic nephropathy in DBA2J mice despite urinary clearance documented by HPLC. BMC Complement Altern Med 10: 67.

Mezzano SA, Barria M, Droguett MA, Burgos ME, Ardiles LG, Flores C et al. (2001). Tubular NF-kappaB and AP-1 activation in human proteinuric renal disease. Kidney Int 60: 1366–1377.

Morimoto T, Sunagawa Y, Kawamura T, Takaya T, Wada H, Nagasawa A et al. (2008). The dietary compound curcumin inhibits p300 histone acetyltransferase activity and prevents heart failure in rats. J Clin Invest 118: 868–878.

Moriwaki Y, Inokuchi T, Yamamoto A, Ka T, Tsutsumi Z, Takahashi S et al. (2007). Effect of TNF-alpha inhibition on urinary albumin excretion in experimental diabetic rats. Acta Diabetol 44: 215–218.

Navarro-Gonzalez JF, Mora-Fernandez C (2008). The role of inflammatory cytokines in diabetic nephropathy. J Am Soc Nephrol 19: 433–442.

Panicker SR, Kartha CC (2010). Curcumin attenuates glucose-induced monocyte chemoattractant protein-1 synthesis in aortic endothelial cells by modulating the nuclear factor-kappaB pathway. Pharmacology 85: 18–26.

Rosemond MJ, St John-Williams L, Yamaguchi T, Fujishita T, Walsh JS (2004). Enzymology of a carbonyl reduction clearance pathway for the HIV integrase inhibitor, S-1360: role of human liver cytosolic aldo-keto reductases. Chem Biol Interact 147: 129–139.

Shanmugam N, Reddy MA, Guha M, Natarajan R (2003). High glucose-induced expression of proinflammatory cytokine and chemokine genes in monocytic cells. Diabetes 52: 1256–1264.

Sharma S, Kulkarni SK, Chopra K (2006). Curcumin, the active principle of turmeric (Curcuma longa), ameliorates diabetic nephropathy in rats. Clin Exp Pharmacol Physiol 33: 940–945.

Shi Y, Du C, Zhang Y, Ren Y, Hao J, Zhao S et al. (2010). Suppressor of cytokine signaling-1 ameliorates expression of MCP-1 in diabetic nephropathy. Am J Nephrol 31: 380–388.

Stan D, Calin M, Manduteanu I, Pirvulescu M, Gan AM, Butoi ED et al. (2011). High glucose induces enhanced expression of resistin in human U937 monocyte-like cell line by MAPK- and NF-kB-dependent mechanisms; the modulating effect of insulin. Cell Tissue Res 343: 379–387.

Tang T, Zhang J, Yin J, Staszkiewicz J, Gawronska-Kozak B, Jung DY et al. (2010). Uncoupling of inflammation and insulin resistance by NF-kappaB in transgenic mice through elevated energy expenditure. J Biol Chem 285: 4637–4644.

Tesch GH (2010). Macrophages and diabetic nephropathy. Semin Nephrol 30: 290–301.

Tikoo K, Meena RL, Kabra DG, Gaikwad AB (2008). Change in post-translational modifications of histone H3, heat-shock protein-27 and MAP kinase p38 expression by curcumin in streptozotocin-induced type I diabetic nephropathy. Br J Pharmacol 153: 1225–1231.

Utimura R, Fujihara CK, Mattar AL, Malheiros DM, Noronha IL, Zatz R (2003). Mycophenolate mofetil prevents the development of glomerular injury in experimental diabetes. Kidney Int 63: 209–216.

Wen Y, Gu J, Li SL, Reddy MA, Natarajan R, Nadler JL (2006). Elevated glucose and diabetes promote interleukin-12 cytokine gene expression in mouse macrophages. Endocrinology 147: 2518–2525.

Xu Z, Lin S, Wu W, Tan H, Wang Z, Cheng C et al. (2008). Ghrelin prevents doxorubicin-induced cardiotoxicity through TNF-alpha/NF-kappaB pathways and mitochondrial protective mechanisms. Toxicology 247: 133–138.

Yonemoto S, Machiguchi T, Nomura K, Minakata T, Nanno M, Yoshida H (2006). Correlations of tissue macrophages and cytoskeletal protein expression with renal fibrosis in patients with diabetes mellitus. Clin Exp Nephrol 10: 186–192.

Yozai K, Shikata K, Sasaki M, Tone A, Ohga S, Usui H et al. (2005). Methotrexate prevents renal injury in experimental diabetic rats via anti-inflammatory actions. J Am Soc Nephrol 16: 3326–3338.

Zhao C, Cai Y, He X, Li J, Zhang L, Wu J et al. (2010). Synthesis and anti-inflammatory evaluation of novel mono-carbonyl analogues of curcumin in LPS-stimulated RAW 264.7 macrophages. Eur J Med Chem 45: 5773–5780.

Zong H, Ward M, Madden A, Yong PH, Limb GA, Curtis TM et al. (2010). Hyperglycaemia-induced pro-inflammatory responses by retinal Muller glia are regulated by the receptor for advanced glycation end-products (RAGE). Diabetologia 53: 2656–2666.

Supporting information

Additional Supporting Information may be found in the online version of this article:

Table S1 Primer sequences for real-time quantitative PCR

Please note: Wiley-Blackwell are not responsible for the content or functionality of any supporting materials supplied by the authors. Any queries (other than missing material) should be directed to the corresponding author for the article.